[redacted]

RM No. L7H26
Copy No. 97

[redacted]

TECH LIBRARY KAFB, NM
0143951

RM L7H26

7105

NACA

RESEARCH MEMORANDUM

FLIGHT INVESTIGATION TO DETERMINE THE HINGE MOMENTS OF A BEVELED-EDGE AILERON ON A 45° SWEPTBACK WING AT TRANSONIC AND LOW SUPERSONIC SPEEDS

By

William N. Gardner and Howard J. Curfman, Jr.

Langley Memorial Aeronautical Laboratory
Langley Field, Va.

CLASSIFIED DOCUMENT

[redacted]

NATIONAL ADVISORY COMMITTEE FOR AERONAUTICS

WASHINGTON
November 12, 1947

[redacted]

319.98/13

Classification cancelled (or changed to Unclassified)

By Authority of NASA Tech Pub Announcement 89 8 Sept 05

(OFFICER AUTHORIZED TO CHANGE)

By .....

.....

GRADE OF OFFICER MAKING CHANGE)

.....10 Apr 6).....

DATE

TECH LIBRARY KAFB, NM
0143951

NATIONAL ADVISORY COMMITTEE FOR AERONAUTICS

RESEARCH MEMORANDUM

FLIGHT INVESTIGATION TO DETERMINE THE HINGE MOMENTS OF A BEVELED-EDGE AILERON ON A 45° SWEPTBACK WING AT TRANSONIC AND LOW SUPERSONIC SPEEDS

By William N. Gardner and Howard J. Curfman, Jr.

SUMMARY

In an effort to determine the reason for loss of roll stabilization at supercritical speeds in flights of the NACA supersonic lateral stability and control research pilotless aircraft RM-1, a model was equipped with a balance to measure aileron hinge moments in flight. The results of the test indicate that the particular aileron design used, 20° beveled edge in combination with $0.52c_a$ overhang balance, had reasonably low hinge moments up to the critical speed range, but as the critical speed was exceeded, the hinge moments first increased quite rapidly and then decreased. At supercritical speeds, however, the hinge moments increased very rapidly. These data add significance to previous conclusions that at subcritical speeds the aileron is overbalanced at δ_a less than 2°, and overbalanced at δ_a less than 4° as the critical speed is exceeded. In the supercritical speed range, however, the aileron very quickly becomes underbalanced over the full deflection range.

In addition, rolling-moment balance data were obtained which indicate that the ailerons experienced a reversal of effectiveness at supercritical speeds. The reversal of aileron effectiveness and resultant failure of the RM-1 to stabilize in roll above the critical Mach number in both the present and previous tests may be primarily attributed to insufficient wing torsional rigidity and to the inability of the servomechanisms employed to maintain the full aileron deflection range.

INTRODUCTION

The purpose of this aileron hinge-moment investigation was to attempt to establish the reason for loss of roll stabilization at speeds corresponding to Mach numbers greater than 0.9 in the flight

of the fifth RM-1 model reported in reference 1. At the time of the fifth RM-1 flight, insufficient information was available to determine whether or not the aileron actually lost its rolling effectiveness or whether the aileron hinge moments were so high that they exceeded the aileron servomechanism power. A standard RM-1 pilotless aircraft, used in lateral stability and control research and described in reference 1, was equipped with a control-position indicator and a balance for measuring the aileron hinge moments. In view of the current interest in control hinge moments through the transonic and into the supersonic speed range, the results of this initial hinge-moment investigation are being presented at this time.

SYMBOLS

δ_a	aileron deflection; positive when producing roll to left, degrees
$b/2$	wing semispan measured normal to fuselage center line, feet
c	wing chord measured in free-stream direction, feet
c_n	maximum wing chord normal to leading edge, feet
c_a	aileron chord measured aft and normal to aileron hinge line, feet
S_a	area of aileron aft of hinge line, square feet
H_a	aileron hinge moment, foot-pounds
q	dynamic pressure, pounds per square foot $\left(\rho V^2/2\right)$
ρ	mass density of air, slugs per cubic foot
V	velocity, feet per second
C_h	nondimensional aileron hinge-moment coefficient $\left(H_a/qS_ac_a\right)$
M	Mach number (V/V_c)
V_c	velocity of sound, feet per second
R	Reynolds number $(\rho cV/\mu)$
μ	coefficient of viscosity of air, slugs per foot-second

APPARATUS AND MODEL

Model

The standard RM-1 stability and control research pilotless aircraft consists of a sharp-nose cylindrical body of fineness ratio 22.7 equipped with cruciform wings and cruciform fins. The wings and fins are of constant chord NACA 65-010 airfoil section normal to the leading edge. Figure 1 is a sketch of the RM-1 model showing its over-all dimensions; and figure 2 is a photograph of a model, equipped with a booster rocket, mounted on its launching rack at the 60° launching angle. The model, booster, and launching equipment are completely described in reference 1.

Two diametrically opposite wings are equipped with ailerons. Figure 3 is a sketch showing the detail dimensions of the wing and aileron. The ailerons are $0.10c_n$ and $0.33(b/2)$. They have an overhang balance of $0.52c_a$ and a 20° beveled trailing edge. The servomechanisms are set to limit the aileron travel to approximately ±10° deflection.

The electromagnetic servomechanisms used to actuate the ailerons function as a flicker-type control, that is, the ailerons are deflected in either one extreme position or the other at all times. The sense of control deflection is determined by a roll-stabilization automatic pilot, identical to the one described in reference 1, except that the rate gyroscope was removed making the automatic pilot a displacement response, flicker-type system.

The load calibration of the servomechanisms employed is presented in figure 4 and is plotted as hinge moment against aileron deflection δ_a. For any given hinge moment the servomechanism was able to hold the aileron at whatever deflection is shown.

Structural tests were made after the flight on wings identical to those used on the model to determine the torsional rigidity of the wing. Torsional moments were applied at the wing tip, and the angular deflection of the midaileron chord parallel to the air stream was measured relative to the center line of the model. These tests show that the torsional stiffness of this laminated spruce wing was equivalent to 230 inch-pounds per degree.

Instrumentation

An NACA telemeter was installed in the model to transmit intelligence on longitudinal acceleration, angle of bank, rolling moment, aileron hinge moment, and aileron position. Reference 1 describes the telemeter equipment and presents a method for obtaining velocity from longitudinal acceleration data. A standard Army-Navy AN/AMQ-1c radiosonde was used to obtain atmospheric pressures and temperatures at the time of the flight.

A control-position indicator and a balance for measuring the aileron hinge moments were installed on one of the aileron servomechanisms. Figure 5 is a photograph of the wing-aileron combination showing the servomechanism, control-position indicator, and the balance for measuring aileron hinge moment.

The two wings with ailerons were rigidly mounted on the free ends of a steel cantilever spring which served as the rolling-moment balance. Reference 2 gives a complete description of the balance system except for two oil-damping units which were added to the system to damp the transient oscillations following a control reversal. This balance measures the summation of the control moment, damping moment, inertia moment, and out-of-trim moment of the two wings with ailerons which were mounted on the rolling-moment balance.

RESULTS AND DISCUSSION

General Flight Behavior

The model was launched successfully and experienced satisfactory booster separation, after which it accelerated to a maximum velocity of 1360 feet per second which corresponded to a Mach number of 1.23. The velocity history of the flight was obtained by integration of the longitudinal acceleration data in accordance with the method presented in reference 1. Velocity was converted to Mach number utilizing atmospheric data obtained from a radiosonde sent aloft at the time of launching. Figure 6 shows the time history of Mach number throughout the entire flight, and figure 7 is a plot of Reynolds number against Mach number.

During the short coasting period after booster rocket burnout and before sustaining rocket ignition, the model stabilized in roll. Shortly after ignition of the sustaining rocket, as the velocity exceeded a Mach number of 0.9, the model lost roll stabilization and rolled continuously over and over throughout the high-speed part

of the flight. As the model lost speed after rocket burnout, the controls again became effective at a Mach number of 0.9, and the model stabilized in roll throughout the remainder of the flight.

Aileron Hinge Moments

Figure 8 is a plot of hinge-moment coefficient per degree aileron deflection against Mach number for the accelerated part of the flight. In interpreting the data shown in figure 8, it must be pointed out that the C_h per δ_a data shown were obtained merely by dividing the measured hinge-moment coefficient by the measured aileron deflection; hence, these data are not an indication of the slope of a curve of hinge-moment coefficient against aileron deflection since, for the type of aileron used, this curve is usually nonlinear.

Up to a Mach number of 0.86 the hinge moments are low and indicate that the particular aileron design used has desirably low hinge moments through the subsonic speed range, at least over a deflection range of $\delta_a = 7^\circ$ to 10°. The sharp increase in C_h per δ_a over the Mach number range from 0.86 to 0.90 is attributed to changes in the pressure distribution as the flow separates from the wing and the boundary layer thickens. The sudden drop in C_h per δ_a at a Mach number of 0.90 is believed to be associated with the rearward movement of the shock on the wing and aileron. In supercritical flow above a Mach number of 0.92, the center of pressure on the aileron moves toward the trailing edge, resulting in the high, undesirable C_h per δ_a shown. These hinge moments were sufficient to reduce the aileron deflection approximately 40 percent.

The data presented herein give added significance to the information obtained from a freely floating aileron, as reported in reference 2. The ailerons in the two cases were identical. Reference 2 shows that the aileron is overbalanced for δ_a less than 2° at subcritical speeds and overbalanced for δ_a less than 4° as the critical speed is slightly exceeded. Both tests indicate a rapid underbalancing tendency over the full deflection range as supercritical velocities are attained.

In utilizing these data it is well to note that the effects of wing stiffness are included. In reference 3 it is shown that reducing the torsional stiffness of a tapered 45° sweptback wing from eight times the stiffness of the RM-1 wing to four times as

stiff resulted in very slight changes in the rolling effectiveness of the full-span, plain-flap controls in the speed range comparable to that of the RM-1. The extremely reduced stiffness of the wing in the present test, due primarily to the large cut-out made to accommodate the servomechanism, may, however, be such as to cause considerable change in the rolling effectiveness and hinge moments of these partial-span ailerons.

Discrepancies in the C_h per δ_a measured with the aileron at alternate up and down deflections are attributed to two primary causes. Although the wing torsional stiffness is known, no accurate information is available on the aileron-hinge normal and chord forces and the pressure distribution over the wing. Consequently, no estimate has been made as to the angle of attack of the wing due to wing twisting and bending; however, the effects of the twist on the hinge moments are believed to be very large and probably unsymmetrical. Also, it is noted in figure 5 that the aileron servomechanism did not have identical power characteristics for the two deflections.

The maximum value of the tip helix angle reached in the flight was 0.009 radian and occurred at subsonic speeds in stabilized flight. This maximum value is believed to be so small that it would have very little effect on the hinge moments measured.

It should be pointed out that, at the Mach number at which serious hinge-moment changes first occur (0.86), sharp drag increases as noted in reference 1 also occur. This fact is substantiated in reference 3, which shows that large drag increases occur at the Mach number at which severe loss in control effectiveness is experienced.

Roll Stabilization

The rolling-moment balance data obtained during the flight show that, in the speed range above a Mach number of 0.90, the effectiveness of the ailerons was reversed.

Figure 9 is a reproduction of two parts of the telemeter record obtained from the flight. The records shown are of aileron position and rolling-moment-balance deflection and show the effect on the rolling-moment balance of a change of aileron deflection. Figure 9(a) is typical for velocities below and figure 9(b) is typical for velocities above those corresponding to a Mach number of 0.90. In figure 9(b), it is noted that the sense of the rolling-moment-balance change is the reverse of that shown in figure 9(a). It should be noted too that, at both instances of figure 9, the model was in a continuous roll, stabilization not yet being established in figure 9(a). The

reversals of the aileron deflections are due to the particular flicker-type automatic pilot used which gives a corrective control for the first 180° of roll, and at 180° will reverse the control which thus tends to restore the model to the zero position through the shortest path.

Because of the relatively low wing stiffness, it is believed that the reversal of aileron effectiveness can be attributed primarily to severe wing twist. This fact probably accounts for the loss of roll stabilization at speeds above a Mach number of 0.90 on both this flight and the one reported in reference 1. However, there are also other factors involved. Of primary importance is the fact that the aileron hinge moments became so high above a Mach number of 0.90 that the servomechanisms were unable to hold the ailerons at full deflection. This fact could result in a control moment-automatic pilot combination unable to overcome out-of-trim conditions. Another factor is the reduction of control effectiveness through the transonic and into the supersonic speed range. Reference 3 presents aileron effectiveness data for plain flaps on 45° sweptback wings which show that there is a large reduction in aileron effectiveness in going from a Mach number of 0.7 to 1.4. It is believed that this would also hold true for the 45° sweptback wing-aileron combination used in the present tests, regardless of the torsional stiffness employed.

CONCLUSIONS

Based on the data obtained from the flight herein reported, the following conclusions may be drawn:

1. The 20° beveled-edge aileron with $0.52c_a$ overhang aerodynamic balance provided reasonably low hinge moments up to the critical speed range but, as the critical speed was exceeded, the hinge moments first increased quite rapidly and then decreased. At supercritical speeds, however, the hinge moments increased very rapidly. These facts add significance to previous conclusions that at subcritical speeds the aileron is overbalanced at δ_a less than 2°, and overbalanced at δ_a less than 4° as the critical speed is slightly exceeded. In the supercritical speed range, however, the aileron very quickly becomes underbalanced over the full deflection range.

2. The reversal of aileron effectiveness and resultant failure of the RM-1 to stabilize in roll above the critical Mach number in both the present and previous tests may be primarily attributed to

insufficient wing torsional rigidity and to the inability of the servomechanisms employed to maintain the full aileron deflection range.

Langley Memorial Aeronautical Laboratory
National Advisory Committee for Aeronautics
Langley Field, Va.

REFERENCES

1. Pitkin, Marvin, Gardner, William N., and Curfman, Howard J., Jr.: Results of Preliminary Flight Investigation of Aerodynamic Characteristics of the NACA Two-Stage Supersonic Research Model RM-1 Stabilized in Roll at Transonic and Supersonic Velocities. NACA RM No. L6J23, 1946.

2. Pitkin, Marvin, Gardner, William N., and Curfman, Howard J., Jr.: Observations on an Aileron-Flutter Instability Encountered on a 45° Swept-Back Wing in Transonic and Supersonic Flight. NACA RM No. L6L09, 1946.

3. Sandahl, Carl A.: Free-Flight Investigation of Control Effectiveness of Full-Span 0.2-Chord Plain Ailerons at High Subsonic, Transonic, and Supersonic Speeds to Determine Some Effects of Wing Sweepback, Taper, Aspect Ratio, and Section Thickness Ratio. NACA RM No. L7F30, 1947.

[redacted]

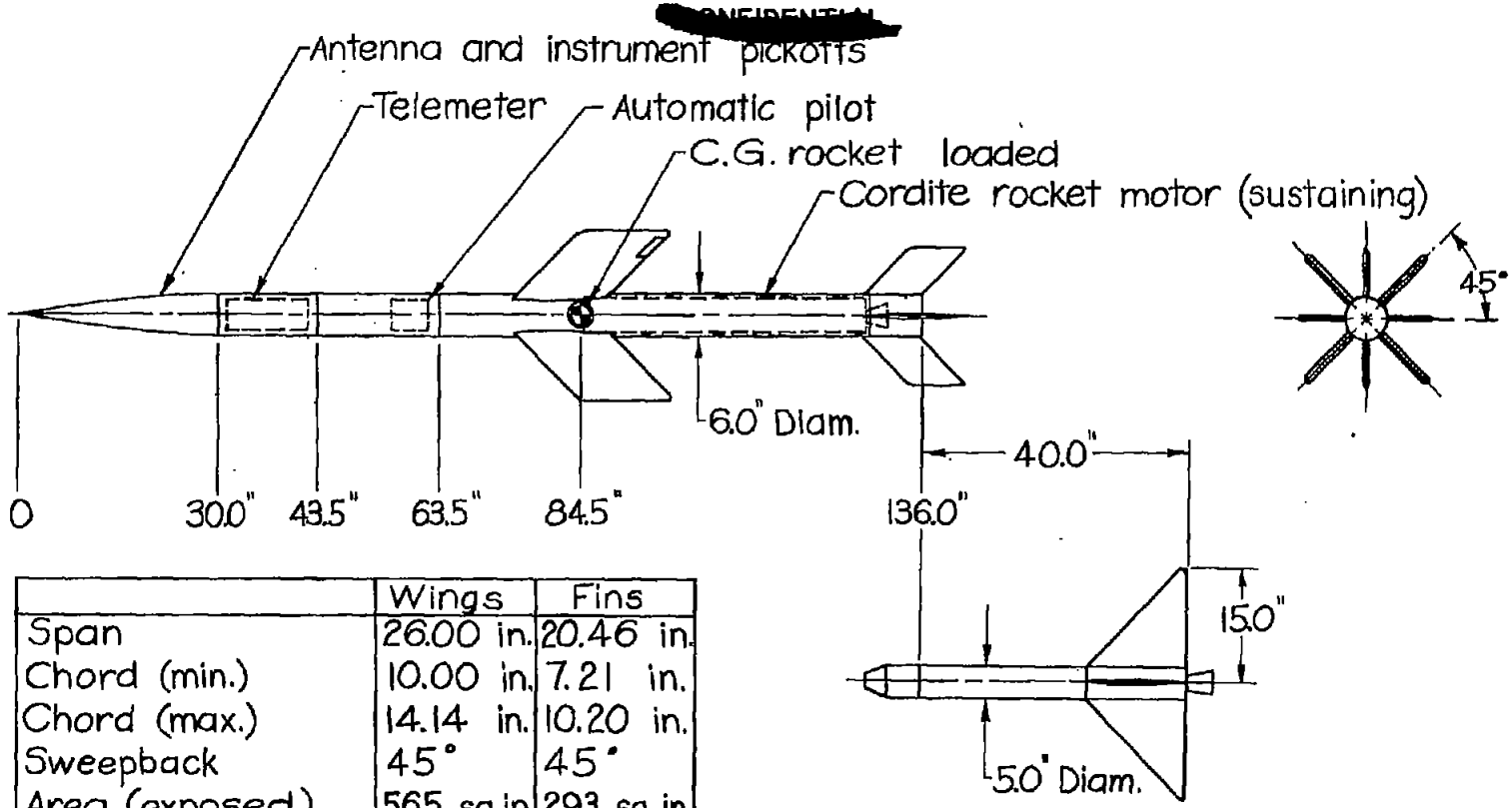

	Wings	Fins
Span	26.00 in.	20.46 in.
Chord (min.)	10.00 in.	7.21 in.
Chord (max.)	14.14 in.	10.20 in.
Sweepback	45°	45°
Area (exposed)	565 sq in.	293 sq in.
Airfoil (min. chord)	NACA 65-010	NACA 65-010
Fuselage		
Length	136 in.	
Diameter	6 in.	
General		
Rocket motor :		
Weight (loaded)	67 lb	
Weight (empty)	40 lb	

[redacted]

NATIONAL ADVISORY COMMITTEE FOR AERONAUTICS

Figure 1.- Over-all design features of the NACA supersonic control-research model , RM-1.

CONFIDENTIAL

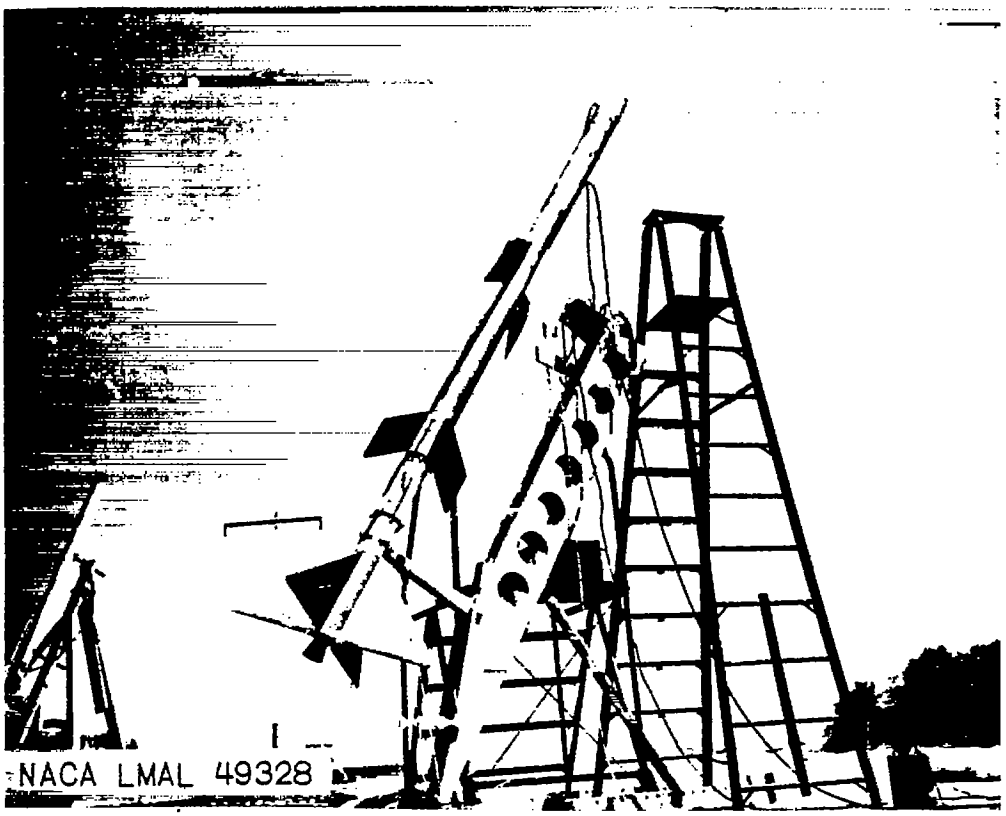

Figure 2.- The RM-1 with booster mounted on launching rack.

CONFIDENTIAL

[redacted]

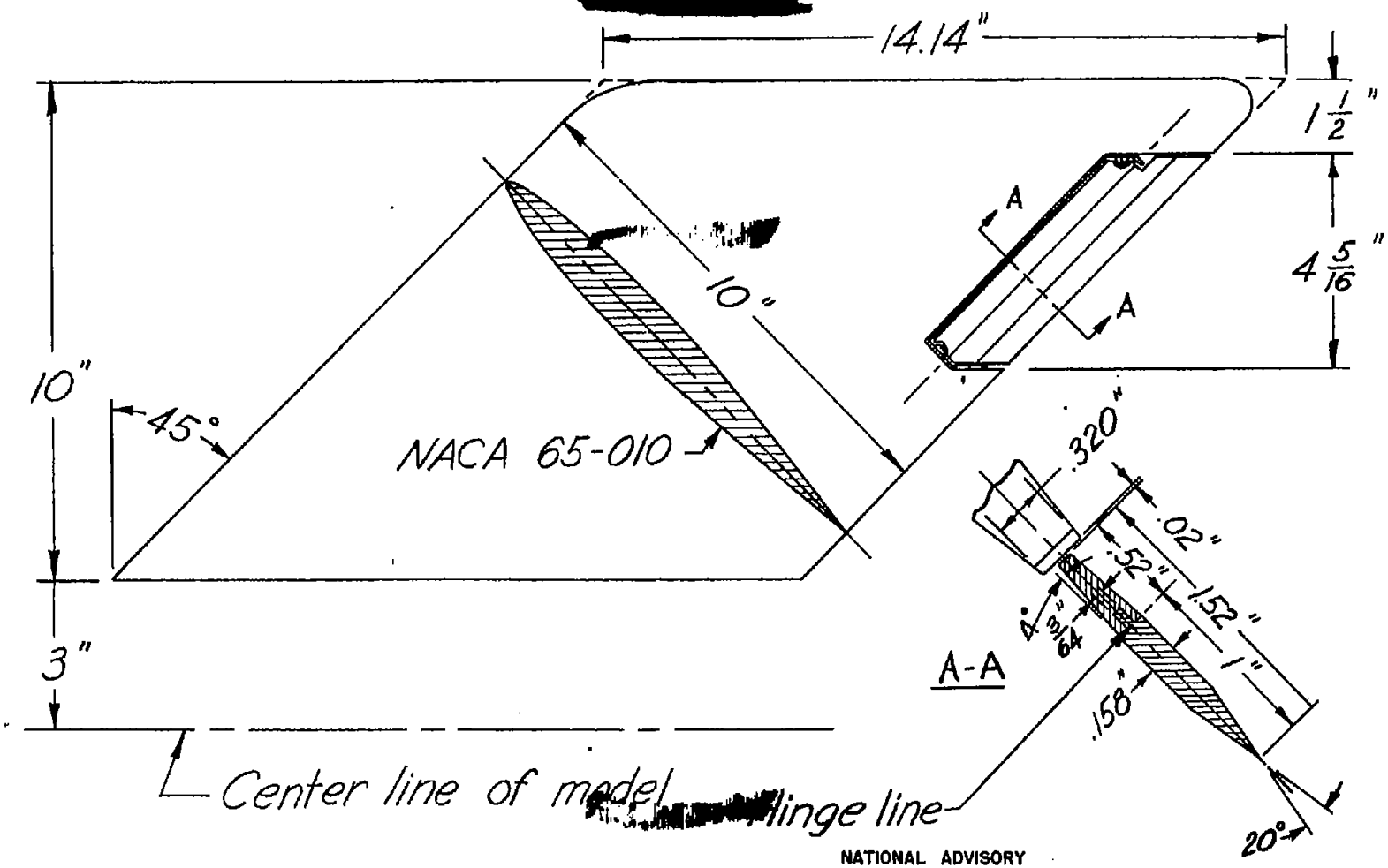

NATIONAL ADVISORY
COMMITTEE FOR AERONAUTICS

Figure 3. - RM-1 wing-aileron detail.

[redacted]

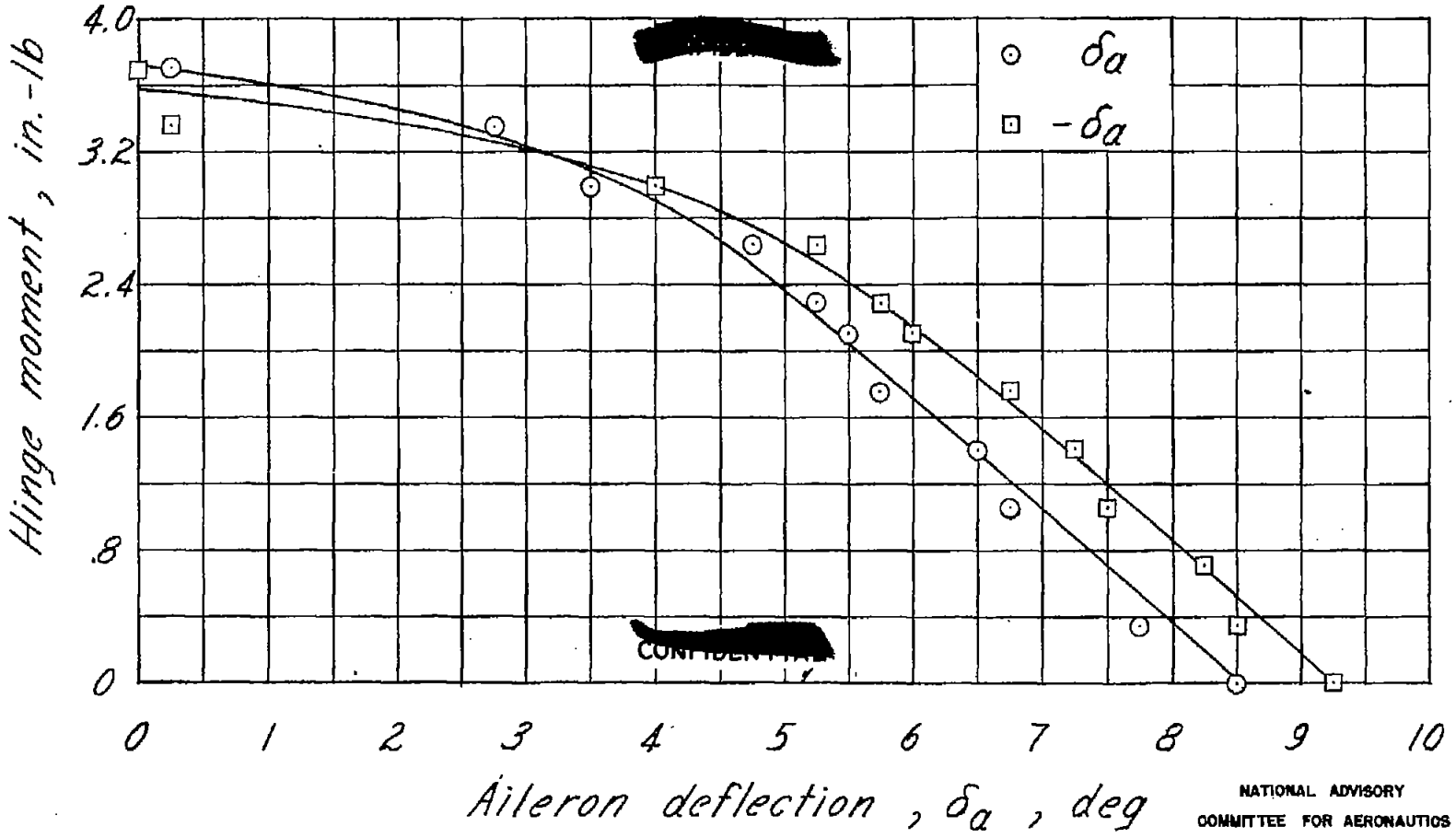

Figure 4.- Load calibrati[redacted] aileron servomechanism.

[redacted]

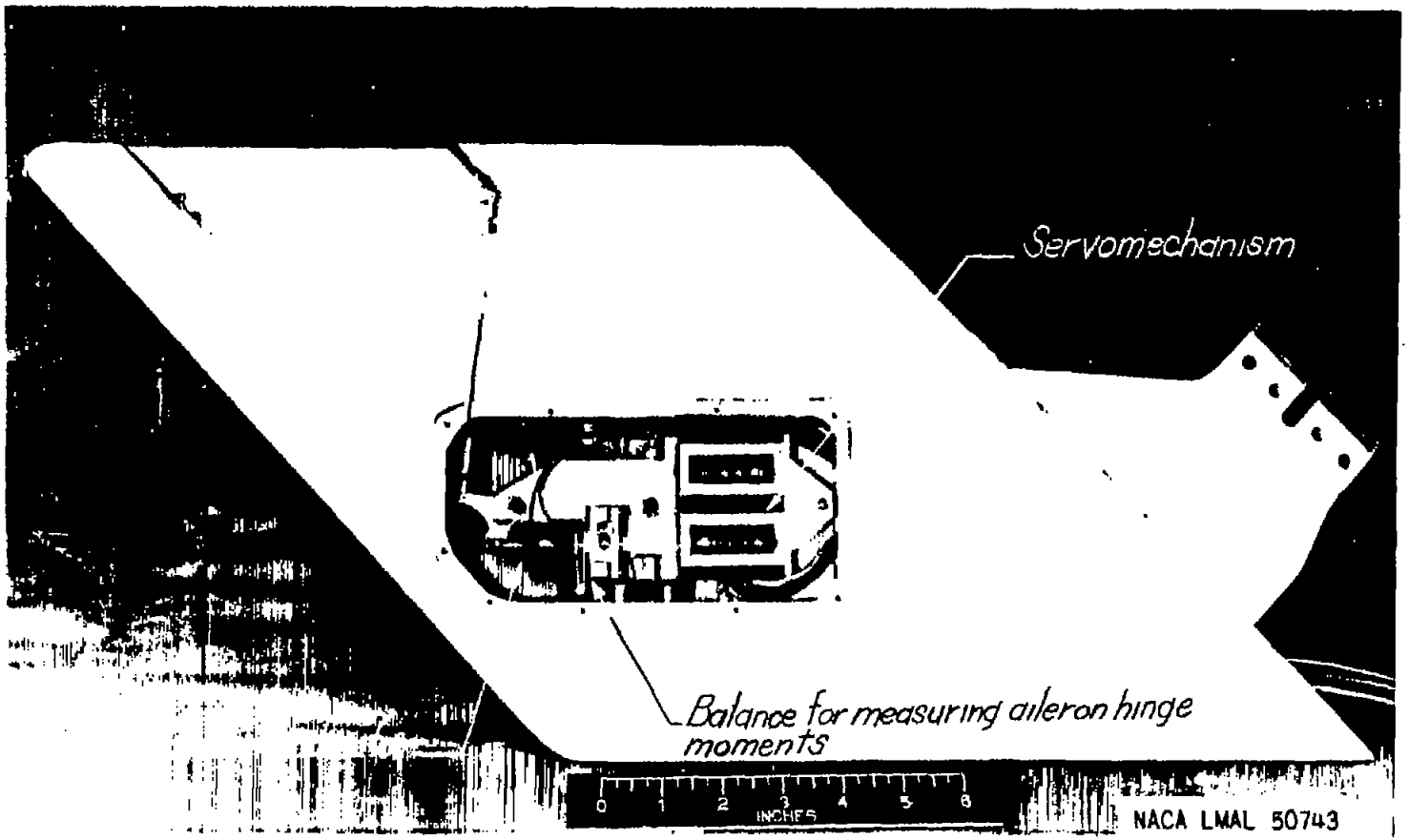

Figure 5.- The RM-1 wing showing aileron hinge-moment balance, servomechanism, and control-position indicator.

[redacted]

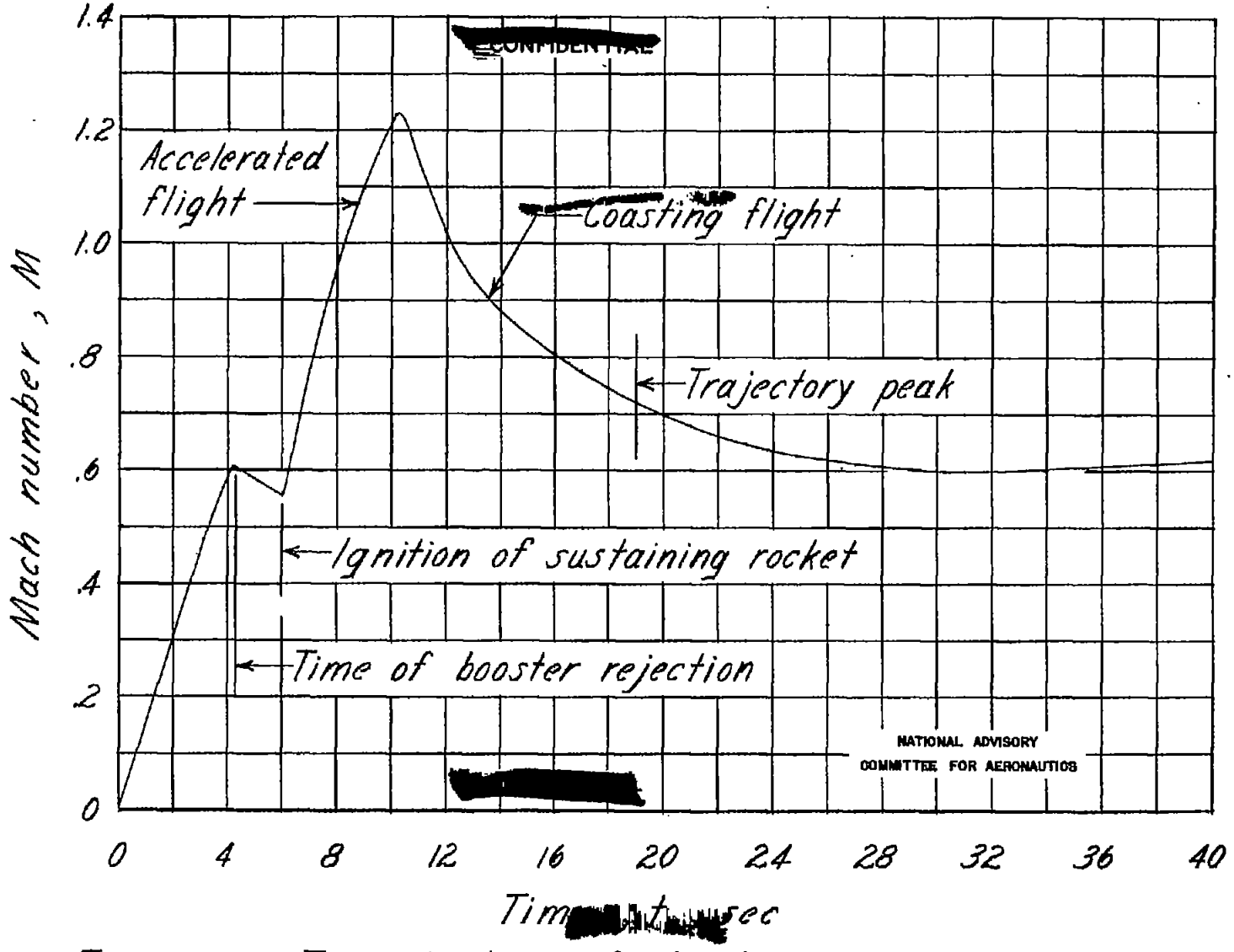

Figure 6.- Time history of Mach number.

[redacted]

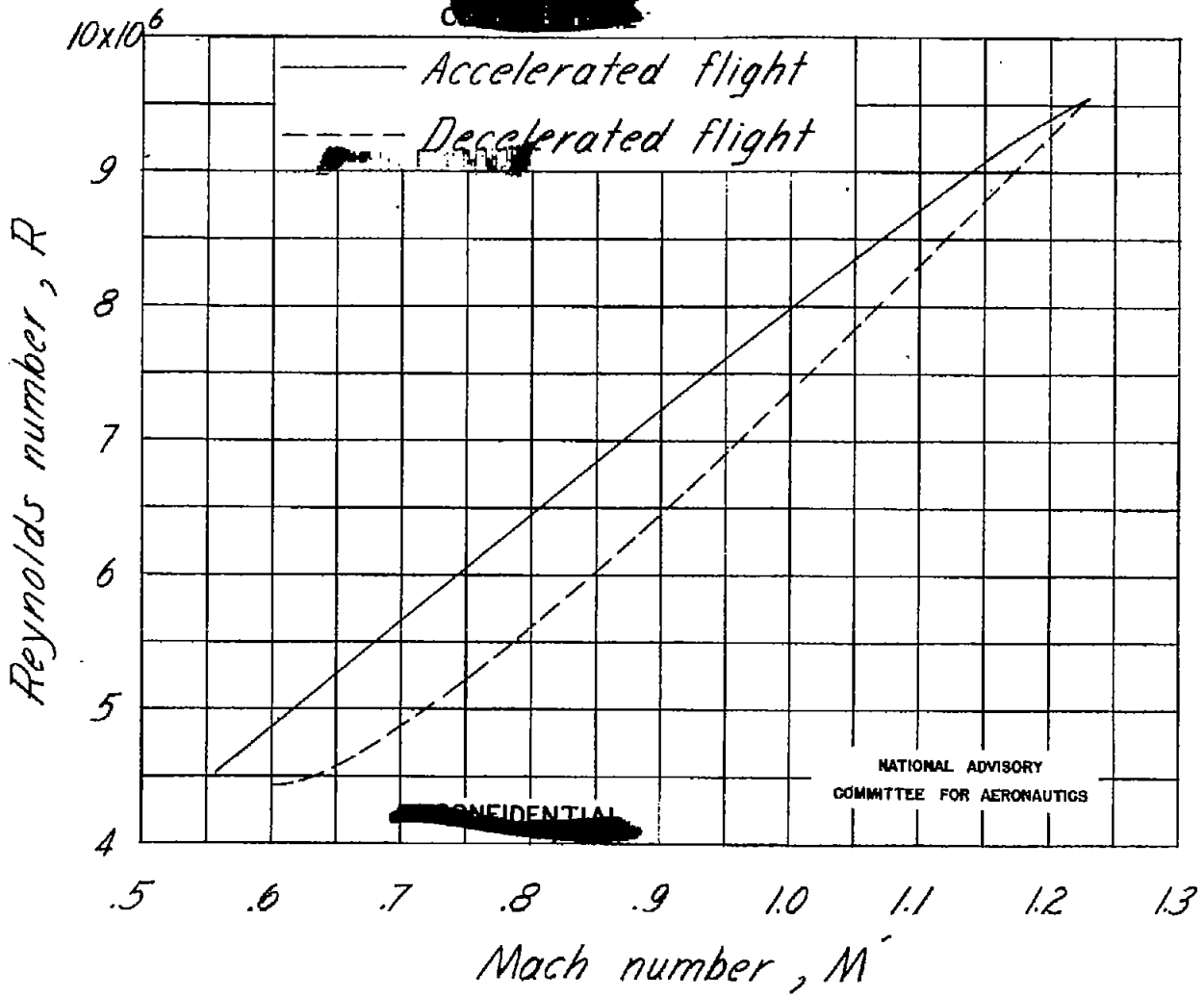

[redacted]

Figure 7.- Reynolds number variation with Mach number.

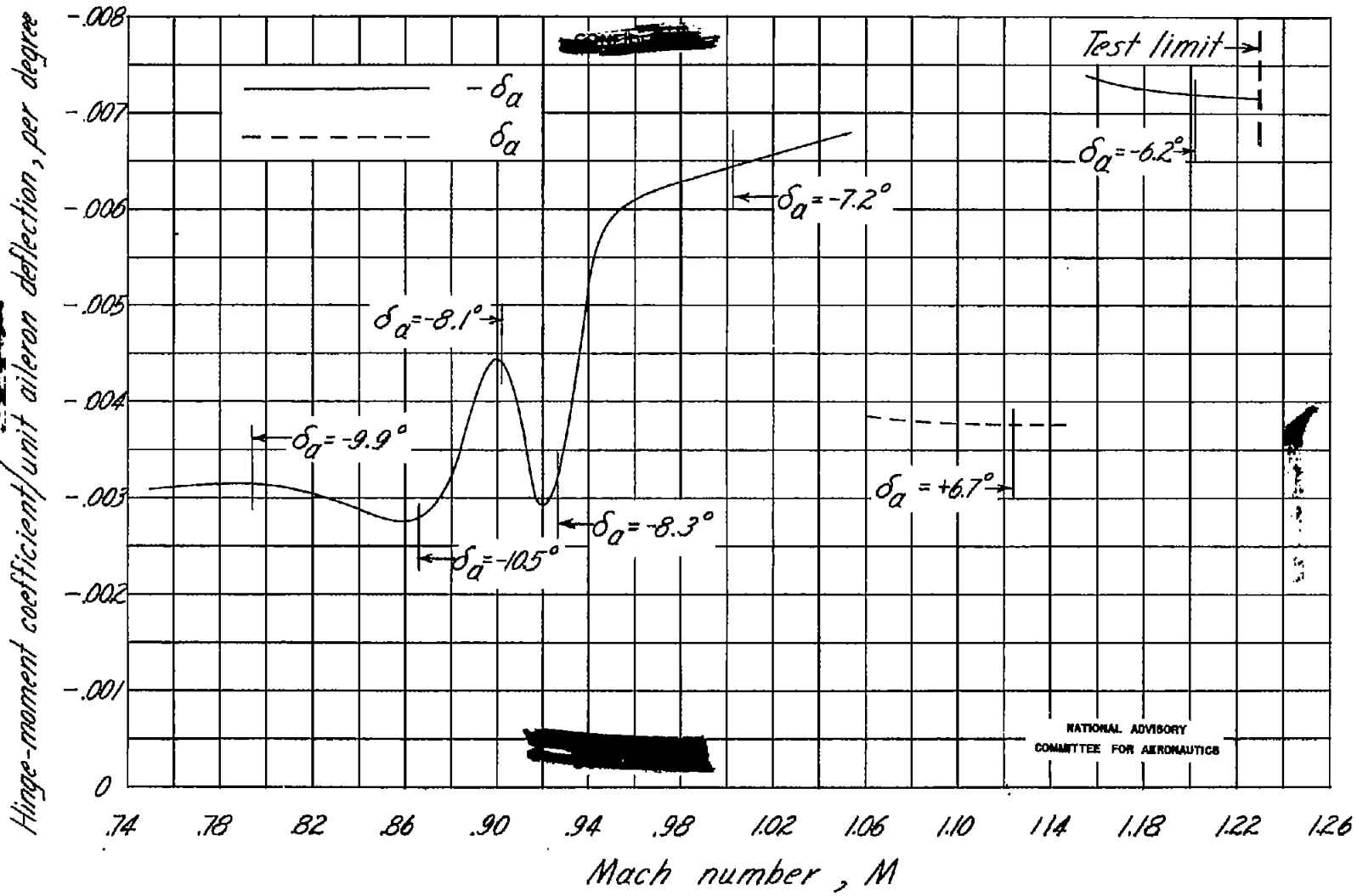

Figure 8.- Hinge-moment coefficient per degree aileron deflection against Mach number.

CONFIDENTIAL

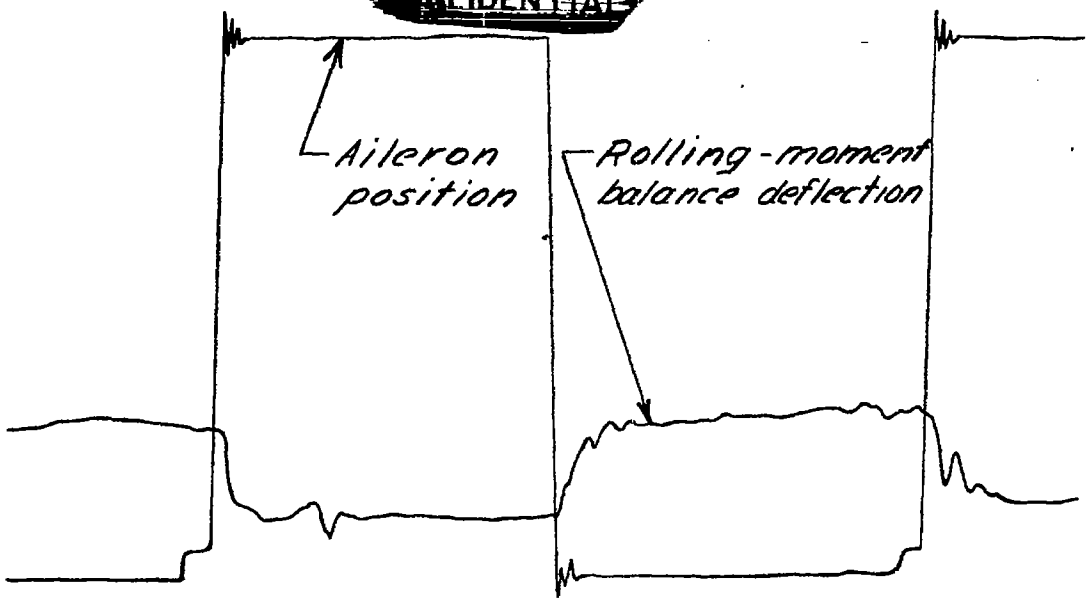

(a) $M < 0.90$.

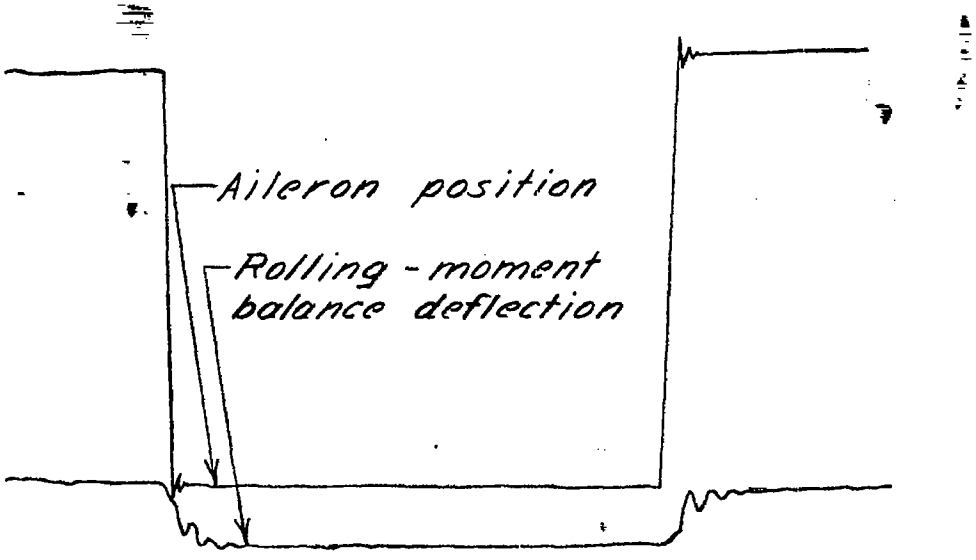

(b) $M > 0.90$.

NATIONAL ADVISORY COMMITTEE FOR AERONAUTICS

Figure 9.- Reproductions of telemeter records showing the reversal of rolling moments produced by aileron deflections at $M > 0.90$.

CONFIDENTIAL